A way to macroporous and alveolar geopolymer foams elaboration: Influence of operating parameters on porosity characteristics

Sara Benkhirat, Gaël Plantard, Enrique Ribeiro, Hervé Glenat, Yonko Gorand, K. Nouneh

▶ **To cite this version:**

Sara Benkhirat, Gaël Plantard, Enrique Ribeiro, Hervé Glenat, Yonko Gorand, et al.. A way to macroporous and alveolar geopolymer foams elaboration: Influence of operating parameters on porosity characteristics. Results in Materials, 2024, 24, pp.100613. 10.1016/j.rinma.2024.100613 . hal-04805611

HAL Id: hal-04805611
https://cnrs.hal.science/hal-04805611v1

Submitted on 28 Nov 2024

HAL is a multi-disciplinary open access archive for the deposit and dissemination of scientific research documents, whether they are published or not. The documents may come from teaching and research institutions in France or abroad, or from public or private research centers.

L'archive ouverte pluridisciplinaire **HAL**, est destinée au dépôt et à la diffusion de documents scientifiques de niveau recherche, publiés ou non, émanant des établissements d'enseignement et de recherche français ou étrangers, des laboratoires publics ou privés.

Distributed under a Creative Commons Attribution 4.0 International License

Results in Materials 24 (2024) 100613

Contents lists available at ScienceDirect

Results in Materials

journal homepage: www.sciencedirect.com/journal/results-in-materials

A way to macroporous and alveolar geopolymer foams elaboration: Influence of operating parameters on porosity characteristics

S. Benkhirat [a], G. Plantard [b,*], E. Ribeiro [b], H. Glenat [b], Y. Gorand [b], K. Nouneh [a,**]

[a] LMPS, Laboratory of Materials Physics & Subatomics, Department of Physics, Faculty of Sciences, Ibn Tofail University, BP 133, Kenitra, Morocco
[b] PROMES-CNRS UPR 8521, PROcess Material and Solar Energy, Rambla de la Thermodynamique, 66100, Perpignan, France

ARTICLE INFO

Keywords:
Geopolymer foam
Macroporosity
Alveolar
Foaming agent

ABSTRACT

Alveolar cellular foams are widely used in a wide range of applications, from aeronautics and filtration systems to chemical and transformation processes. Their porous characteristics make them a prime candidate for reactions, radiative transfer and flow. Geopolymeric foams, which have their origins in civil engineering, are materials with promising potential in terms of mechanical, thermal and acoustic resistance. As they are mainly used in civil engineering, the structures currently being developed are mainly closed-pore matrices. However, if they are to invert the field of photocatalytic oxidation processes, solar collectors or concentrated solar power plants, the supports need to develop a high exchange surface area. Metal alveolar foams have been identified as ideal but very costly supports. Geopolymeric foams could meet these requirements, but their surface areas are currently too limited for photoreactors. In this study, it is proposed to develop and optimize the operating conditions for geopolymer foam synthesis in order to impart macroporous properties and an interconnected alveolar structure. Based on two well-established synthesis methods (direct foaming and replication), operating conditions such as foaming agent and surfactant content, and drying and calcination conditions, are studied. Geopolymer foams are produced with different macroporous characteristics. We aim to define the synthesis conditions required to produce interconnected macroporous alveolar foams with milimetric pores. In civil engineering, these materials have the advantage of being easy to design, use and shape according to the application.

1. Introduction

In the field of solar engineering, photoreactors are used in a wide range of applications, including bioreactors for algae production [1], advanced oxidation processes for water treatment [2,3,4], conversion processes for solar fuel production [5], and receivers for solar tower power plants [6]. Advanced oxidation processes such as heterogeneous photocatalysis that enable photons to be photo-converted into chemical energy are based on the principle of photo-excitation of a catalyst by solar radiation [7]. However, development of these technologies is held back by this issue of how to manage the solar resource [4], which is discontinuous on several scales due to daily and seasonal cycles and meteorological conditions. These major obstacles call for the development of solutions to optimize the use of solar irradiation.

The best way is shaping photocatalytic materials with very high exchange-surface areas in order to make substantial gains in terms of heat transfer intensification, mixing, radiative and reaction transfers [8]. The development of alveolar foams is a promising way for many solar applications [7,9,10]. Functionalized with a photocatalyst, these supports can perform on a level similar nanocatalyst suspensions, which are the reference material [7,11]. Generally speaking, they feature a macroscopically porous (75 %–90 %), low-density, three-dimensional structure with a high degree of interconnection, which lends them huge versatility for shapability. Their chaotic, disordered architecture results in specific surface areas of the order of 10–50 $m^2\ g^{-1}$, which dramatically increases their ability to scatter radiation [12]. The characteristics of the foams, such as geometry, pore-size distribution and mesh density, can be adapted and tuned to the intended application with the aim of developing the largest possible irradiated surface area, expressed in m^2 of capture surface per m^3 of reactor volume [7,13,14]. At present, the foams being developed are metallic foams, which are too expensive for water treatment applications for example [7], and polymeric foams, which pose a problem of aging due to radical attacks that alter the carbonaceous matter [10]. One of the challenges is to develop low-cost

* Corresponding author.
** Corresponding author.
E-mail addresses: plantard@univ-perp.fr (G. Plantard), khalid.nouneh@uit.ac.ma (K. Nouneh).

https://doi.org/10.1016/j.rinma.2024.100613
Received 20 May 2024; Received in revised form 16 July 2024; Accepted 22 August 2024
Available online 30 August 2024
2590-048X/© 2024 CNRS. Published by Elsevier B.V. This is an open access article under the CC BY license (http://creativecommons.org/licenses/by/4.0/).

macroporous alveolar foams with modular porous properties enabling optimal use of the solar resource.

In a context of sustainable development and appropriate technology, geopolymers are an innovative alternative in terms of reusability, durability [15], CO_2 emissions and energy consumption [16]. Thanks to their mechanical properties, low permeability, and thermal and chemical resistance, they find many applications, particularly in civil engineering [17,18]. Geopolymers can be manufactured from natural aluminosilicate minerals (metakaolin) or industrial wastes (fly ash) mixed with aqueous solutions containing basic reactive ingredients, typically sodium hydroxide or potassium/sodium silicates [19].

Scientists have recently turned to investigate the use of geopolymer foams, which are attracting growing interest due to their ability to increase porosity and exchange surface while preserving their original properties [20,21]. This development opens up new fields of application as membrane supports, coatings, adsorbents, filters, or photocatalytic supports [28]. Geopolymer foams can be prepared by impregnating replicas foams with geopolymer pastes (the 'replication' method) [22,23]. There are numerous techniques based on replication, impregnation, matrix reinforcement, and grafting of post-elaboration functionalities that are detailed in the literature [24–27]. The replication route has been recognized as a facile approach for porous geopolymers characterized by interconnected open porosity [24]. Open-cell foams can thus be synthesized by an easy replication route using polymer foams as templates. The support is then impregnated using geopolymers as precursors [25,28]. The result is durable, high value-added materials with a modular porous structure [29]. The porous characteristics cover a wide range, from open-pore honeycomb structures to interconnected pore networks and millimetric pore sizes [24,26,30]. These structures can then be functionalized to confer specific properties (adsorption, thermal, mechanical) to cover a wide range of applications. Geopolymer foams can also be elaborated by adding foaming agents to geopolymer pastes (the 'direct foaming' method). Hydrogen peroxide is the foaming agent of most interest for the design of high-porosity geopolymer foams [31,32]. The decomposition of hydrogen peroxide is an uncontrolled reaction that gives rise to the formation of a highly heterogeneous porous matrix of particular interest for photocatalysis applications. Furthermore, work has shown that presence of surfactant, alkaline activator, and drying temperature also play a key role in developing highly-porous geopolymer foams. For example, high alkalinity appears to promote the hydrogen peroxide decomposition reaction whereas a sodium silicate solution tends to stabilize it [33]. Palmero et al. [34], recently applied different operating conditions, i.e. varying the amount of hydrogen peroxide and the type of geopolymer mixture, and confirmed that this route holds interest for modifying the porous properties of geopolymers. Novais et al., carried out further research by modifying various parameters such as peroxide concentration and NaOH molar ratios during the synthesis of geopolymer foams [35]. These studies show that as the geopolymerization and foaming reactions are coupled, different operating conditions which influence both reaction processes, lead to very different porosity characteristics. Although much work has been published on the synthesis of geopolymer foams, further research is still needed in order to control and increase porosity and confer an interconnected macroporous or alveolar structure with a well-controlled pore distribution.

Here we report research designed to develop macroporous geopolymer foams with an interconnected alveolar structure adapted to solar applications. These characteristics are sought to promote radiative transfer, facilitate fluid flow in the network and develop exchange surface area for reactions. The first part is devoted to testing the direct foaming method and the replication method by modulating key conditions studied in the literature. We modulated the levels of the constituents over a very wide range of values and to the limit of what has been studied in the literature, so as to achieve geopolymer foams with properties tailored to the intended application. Secondly, mechanical strength, composition, structure and mesoporosity of geopolymer foams are studied to control that their properties are in line with those in the literature. In a last and main step, this article aim to highlight the most favorable elaboration conditions for giving geopolymer foams an open-cell structure, high porosity and millimetric pore size. Our approach is to correlate the key operating conditions, such as type of replica, foaming agent rate, surfactant type and rate, and drying conditions, to the porous characteristics. The focus will be on porosity characteristics such as pore-size distribution, pore fraction and type of pore structure (closed, open, honeycomb alveolar) using image processing. The aim is to highlight the method and operating conditions to obtaining the desired properties. Particular attention is paid to the design of macroporous geopolymer foams that develop an interconnected open alveolar-type structure with millimetric pore sizes.

2. Materials and methods

2.1. Elaboration de geopolymer foams

Based on two robust methods studied in the literature, the aim is to develop a wide range of geopolymer foams. The idea is to impart porous properties meeting the criteria of macroporosity, interconnected honeycomb network and millimetric pores. To achieve this, the operating conditions of the production process will be tested to modulate the porous properties.

2.1.1. Geopolymer synthesis

The synthesis of geopolymers by alkaline activation of an aluminosilicate material can be obtained by mixing a strongly basic liquid with an amorphous solid particle system material in molar ratios ranging from 0.2 to 1 [36]. As the solid particles solubilize on contact with the alkaline solution, they release aluminates and silicates in the form of monomers [37]. These monomers combine to form structures called polysialates, with the sialate corresponding to the silicon-oxo-aluminate base block, that cross-link via an Si-O-Al bridge. These amorphous three-dimensional aluminosilicate structures are classified in the 'geopolymers' family. The synthesis of geopolymers depends on several parameters, including the precursor materials (composition, quantity, particle size), the alkaline agents (nature, content), and the calcination conditions (temperature, duration, pre-drying). These factors, which influence geopolymer hardness, have been studied in an effort to understand their role in the formation and characteristics of geopolymers [38–41].

For this study, the geopolymer paste was prepared using a standard composition from the literature [21,42,43]. The alkaline solution was prepared from a solid activator sodium hydroxide (Aldrich, 99.9 %) and sodium silicate (Sigma-Aldrisch, 75 % SiO_2/23.3 % Na_2O) to obtain a solution with a NaOH concentration of 8M and a Silicate concentration of 11.05M. The 1 L solution was stirred for 24 h. Metakaolin (MK) Al_2O_3, $2SiO_2$) was then added and mixed for 10 min to obtain a smooth, homogeneous paste.

2.1.2. Procedure for forming geopolymer foams

Geopolymer foams were developed by two methods: the direct foaming technique and replication. The direct foaming method, which is the most widely used [21], consists of introducing a foaming agent into the fresh geopolymer paste. The most widely used foaming agent, the choice of which was conditioned by the formation and drying time, is hydrogen peroxide [44]. Its decomposition in an extremely basic environment leads to the formation of a complex cellular matrix. The high alkalinity favors the decomposition of hydrogen peroxide, while the sodium silicate solution stabilizes the foam [33].

For this study, the production of geopolymer foam by direct foaming was carried out with the procedure illustrated in Fig. 1. The same conditions as for the preparation of geopolymer paste (section I.1) were applied to produce a foam that will serve as a reference for this study [21,42,43]. For one sample preparation, a 5 ml volume of previously

prepared alkaline solution was poured into a beaker with 0.1 g of surfactant added using a pipette and mixed with a spatula for 5 min. Then 0.5 ml of hydrogen peroxide (30 % concentration) was injected and mixed for 2 min. Foaming started as soon as the foaming agent was added and continued for 1 h, and the unconsolidated geopolymer foam was then dried at 40 °C for 24 h. The consolidated foam was then calcined at 800 °C for 2 h. This procedure serves as a reference for the other samples prepared with different mixing and processing conditions, as presented in section I.3 (Table 1).

The replication method aims to produce macroporous geopolymer foams with an open cell structure and pore sizes ranging from 200 µm to more than 3 mm [45]. Geopolymer foams are developed by impregnating plastic foams with the geopolymer paste, then drying and calcinating [43] the foam under the same conditions as described above. Polyurethane (PU) and polyethylene (PE) foams with dimensions of 50/50/2 mm were chosen as the support. The PU foam has an open cellular structure with a pore size distribution ranging from 0.2 mm to 2 mm. The two PE foams had pore sizes below 2 mm (medium-sized pores, PEM) and between 0.5 and 2 mm (large-sized pores, PEL), respectively. The substrates were impregnated five times for 1 min each time in the reference geopolymer paste described in section I.1. The geopolymer-coated substrates were then allowed to dry for 24 h at 40 °C, then calcined for 2 h at 800 °C.

2.1.3. Operating conditions studied

The synthesis parameters were modulated in an effort to impart macroporosity to geopolymer foams. Each parameter was studied over a wide range in order to identify the parameters that control the key porosity characteristics. The focus was on 1. The surfactant, to stabilize and modulate the size and homogeneity of the bubbles during foaming, 2. foaming agent, to modify the porosity characteristics, and 3. drying conditions, to consolidate the structure.

In general, concentrated alkaline activators allow higher proportions of the Si and Al present in the base precursors to be released and activated to form proportion-mixed geopolymer compounds. Furthermore, a high concentration of the alkaline solution enhances the hardness of the geopolymers by increasing the proportion of silica in the matrix [46]. As the geopolymerization and chemical foaming reactions take place simultaneously during the synthesis of a geopolymer foam, the concentration of the alkaline solution was kept fixed for all experiments to serve as a reference for defining the proportions of the other components (Table 1).

The foaming agent is the key parameter for generating porosity within the geopolymer paste [43,47]. It is possible to control the quantity of foaming agent in order to obtain more aerated macroporous structures. In order to modulate the pore size, porosity and type of porous structure, the proportion of foaming agent was studied over a range from 0.05 ml to 5 ml of H_2O_2, corresponding to foaming agent/alkaline solution ratios ranging from 0.01 to 0.8. Only stable geopolymer foams with sufficient mechanical strength were retained and reported in Table 1. Foams prepared with volumes of foaming agent greater than 5 ml were not mechanically strong enough to be studied.

Surfactants help to stabilize bubbles during the foaming process and influence pore volume and pore size distribution by lowering the surface tension at the gas–liquid interface [48]. Surfactants can thus lead to the formation of different close cell foams, open cell foams, and cellular pore structures. Of the various surfactants studied [42,48], sodium dodecyl sulfate (SDS) and cetyltrimethylammonium (CTAB) are candidates for controlling the microstructure while preserving foams physical and mechanical properties. For this study, two surfactants were studied over a range from 0.01 to 0.3 g of surfactant, corresponding to surfactant/alkaline solution ratios ranging from 0.002 to 0.06 (Table 1).

Drying temperature affects the geopolymer foaming process. A high temperature catalyzes the redox reactions of the foaming agents [49]. During chemical foaming, wet drying conditions above ambient temperature favor the formation of pores with a homogeneous pore-size distribution [50]. Here we tested different drying temperatures ranging from 25 °C to 80 °C in an effort to obtain homogeneous structures (Table 1).

2.2. Characterization techniques

2.2.1. Porous properties

The size and shape of the synthesized geopolymers were analyzed by scanning electron microscopy (SEM-FEG, Hitachi S-4500). Images were acquired with a secondary electron detector and a 5 kV electron beam, at

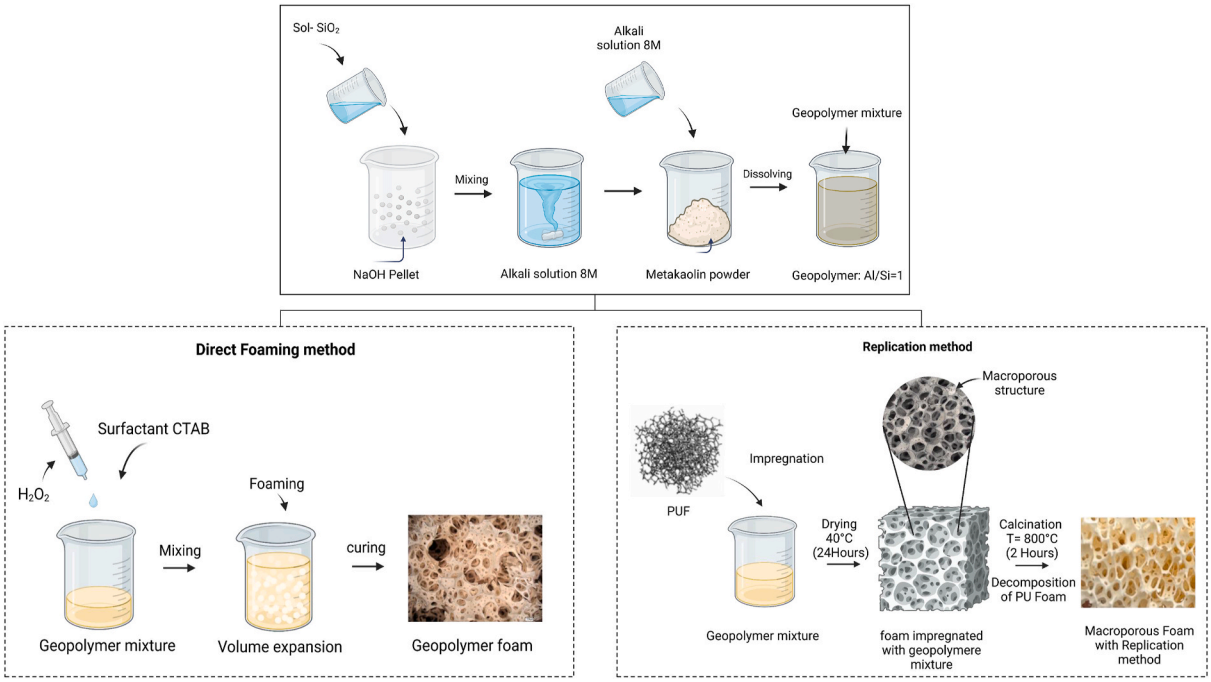

Fig. 1. Route for geopolymer gel synthesis and the two routes for obtaining geopolymer foams, i.e. the direct foaming method and the replication method.

Table 1
Experimental conditions applied to the elaboration of foams by the direct method and characteristics of geopolymer foams.

Samples	Foams samples					
	Foaming agent (ml)	Surfactant (g)	Surfactant/alcaline solution (−)	Foaming agent/alcaline solution (−)	Porosity (−)	ρ (Kg/m3)
Foam 1 (H2O2)	0.05	0.1	0.02	0.01	0.03	2540
Foam 2 (H2O2)	0.2	0.1	0.02	0.04	0.06	2455
Reference Foam	0.5	0.1	0.02	0.1	0.32	1800
Foam 3 (H2O2)	1	0.1	0.02	0.2	0.5	1300
Foam 4 (H2O2)	3	0.1	0.02	0.6	0.75	635
Foam 5 (H2O2)	4	0.1	0.02	0.8	0.8	522
Foam 6 (CTAB)	0.2	0.01	0.002	0.04	0.17	2168
Foam 7 (CTAB)	0.2	0.05	0.01	0.04	0.66	888
Foam 8 (CTAB)	0.2	0.1	0.02	0.04	0.58	1097
Foam 9 (CTAB)	0.2	0.2	0.04	0.04	0.42	1515
Foam 10 (CTAB)	0.2	0.3	0.06	0.04	0.33	1750
Foam 11 (T°C)	0.2	0.1	0.02	0.04	0.19	2116
Foam 12 (T°C)	0.2	0.1	0.02	0.04	0.78	574
Foam 13 (T°C)	0.2	0.1	0.02	0.04	0.7	783
Foam 14 (CTAB)	0.2	0.1	0.02	0.04	0.6	1045
Foam 15 (SDS)	0.2	0.1	0.02	0.04	0.7	783

a working distance of 5 mm. A × 50,000 magnification was used to observe the geopolymer surfaces (Fig. 2). The surface of the geopolymers presents a homogeneous microstructure in the gel form [52]. The surface is bloodless with an ordered structure that may indicate the presence of metakaolin or unreacted precursors. This gel-like microstructure indicates that the geopolymerization reaction was complete [51]. At lower magnifications, the images show the presence of asperities, nodules, and small-scale pores.

In order to define the mesoporous network of geopolymers, characterizations were carried out on the reference geopolymer foam (Table n°1) using a mercury intrusion porosimeter (micrometrics, autoporeIV). The mercury porosimetry analysis technique is based on the intrusion of mercury into a porous structure under rigorously controlled pressures. Mercury porosimetry operates in a pressure range from 0 to 400 MPa, enabling the description of pores with equivalent diameters of between 350 and 0.003 μm. It can be used to calculate pore size distribution, total pore volume, total pore surface area, median pore diameter and sample densities. Analysis is performed in two stages: (1) the penetrometer-sample assembly is in low-pressure configuration (primary vacuum down to 2 bar); (2) then, the penetrometer-sample assembly is in high-pressure configuration (measurement up to 4000 bar). This technique provides information on the mesoporous network, which is complementary to the macroporosity (millimetric porosity) defined by image processing.

In order to evaluate the macroporosity characteristics of geopolymer foams, we set up a three-step methodology see Ref. [52]. For each foam, a series of ten images was taken using a high-resolution optical microscope (VHX Digital Microscope), coupled with software, allowing a magnification of × 2000. All the images were processes with adjustments such as contrast (100 %) and brightness (70 %) to accentuate the differences between the porous zones and the material zones.

The ImageJ freeware, which is classically used for particle size determination and counting, was used to define the porosity characteristics, i.e. pore area and pore number [53]. The scanned image is first reduced to an 8-bit image and then the levels are thresholded. This step is crucial for delimiting the different cells. Reflections on the surface of the cells, which appear as white spots, the eliminated using the “fill holes” procedure. The cells are then separated using the "watershed" procedure in ImageJ, and the pore detection analysis is started. After calibration, the image processing algorithm can produce a file listing the various 2D geometric characteristics of the pores (surface, number, total surface).

Finally, the data is imported into a spreadsheet to classify it by size class. Assuming that the pores are assimilated to circles, the equivalent diameters are calculated from the surfaces and classified by steps of 20 μm. The pore area is calculated from the ratio of total pore area to total area. Statistics, pore-size distributions, and surface areas are determined from more than 1000 pores.

2.2.2. *Mechanical properties*

The mechanical properties of the samples were measured with a nanoindenter equipped with a Berkovich tip (NanoIndenter II, Nano Instruments Inc.). The samples were coated in resin and then polished to ensure that they had a surface finish compatible with the nanoindentation test. The samples (calcined geopolymer and non-calcinated geopolymer) were tested with a maximum applied load of 100 mN, in order to minimize the effect of surface roughness on the measurement caused by the formation of large indentations. The other specimens with thin reticular walls were tested with a maximum applied load of 1.5 mN. The indenter used in these tests is a three-sided pyramid, called a

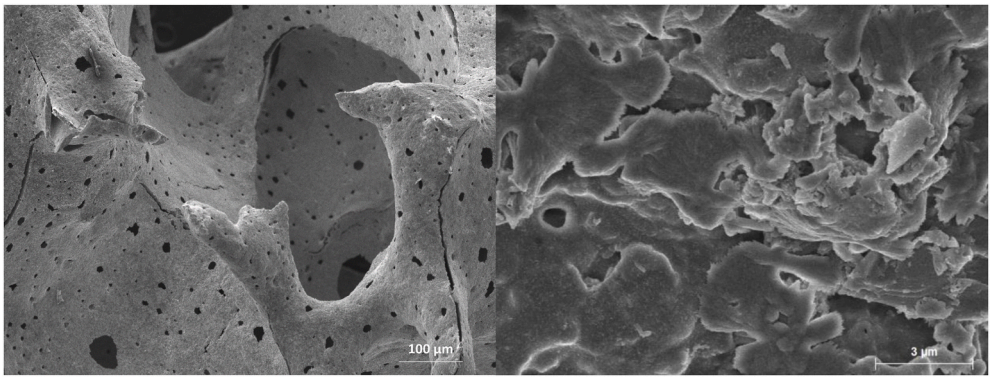

Fig. 2. Surface texture and pores of a geopolymer foam (reference foam) observed by SEM at high magnification (50,000).

Berkovich indenter. The geometric self-similarity of this indenter guarantees a constant hardness measurement regardless of the force applied to the indentation, provided that the material under test is homogeneous at the scale of the nanoindentation measurement. The experimental curves from the tests express the indentation of the indenter tip into the material as a function of the load or force applied to the indenter. The maximum load is kept constant for 10 s in order to take into account possible creep phenomena. The hardness measurement and Young's modulus are extracted from these measurements using the Oliver & Pharr analysis method [54,55].

2.2.3. Composition and structural analysis

A structural characterization was conducted by X-Ray diffraction (XRD) to verify the structure of the synthesized geopolymers. The geopolymer foam was reduced to a powder and analyzed by XRD at room temperature using a PANalytical XPert Pro powder diffractometer (Cu-Kα radiation at λ = 1.5418 Å, 40 kV and 40 mA). The spectrum obtained covers the angular range of 10°–120°. Step size was 0.01 and time per step was 20 s. The diffraction spectrum was recorded and studied using the PANalytical software. The instrumental function can be expressed by a polynomial function and was determined using the SRM 660 reference material (Lanthanum hexaboride, LaB_6 polycrystalline sample).

A Setsys Evolution device (KEP Technologies) was used to perform simultaneous mass variation and heatflow measurements, which were recorded and analyzed using Set Soft software. An experiment was carried out on the geopolymer foam between 25 °C and 800 °C. The heating rate was 10 °C/min with N_2 gas purge.

2.3. Properties of the geopolymer foams

Prior to the study of macroporous characteristics, this section is dedicated to defining the mechanical, microporous, compositional and structural properties of geopolymer foams. The idea is to verify that geopolymer foams developed under different conditions correspond to the standard properties obtained in the literature.

2.4. Analysis of porous characteristics

Firstly, mesoporosity was determined by mercury intrusion porosimetry on a reference foam. In Fig. 3, the pore size distribution shown the presence of two pore size categories: nanopores and micropores. This bimodal distribution is centered on an average diameter of 0.7 μm and 98 μm for nanopores and micropores respectively. Pore volumes correspond to 0.3 ml.g-1 for nanopores and 0.22 ml.g-1 for micropores. The

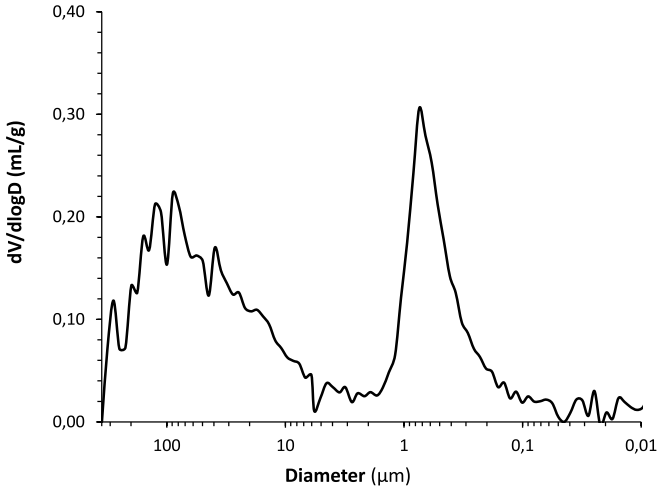

Fig. 3. Pore size distribution by volume of geopolymer foam (reference foam) synthetized by the direct foaming method.

mesoporous structure of geopolymer foams, dominated by capillary pores in the range 0.7 μm–98 μm, is similar to the structures of zeolites [56–58]. It is characteristic of geopolymeric materials that have not been subjected to a foaming process [43,47,73]. It should be noted that, in the context of this study, macroporous properties corresponding to millimeter-sized pores are sought.

The main aim of this study was to define the conditions for obtaining macroporous cellular geopolymer foams. Macroporosity, corresponding to pore sizes in excess of 1 μm, was studied by image processing, in order to identify the influence of processing conditions (temperature, foaming agent, surfactant) on macropore classes.

Fig. 4 shows the geopolymer foam surfaces obtained with different foaming agent volumes (from 0.05 to 4 ml). The pictures show that the foaming agent induces deep modifications in pore structure as it modulates the type of porosity. For small quantities (v = 0.05 ml), the pores are closed, relatively evenly sized, and relatively homogeneously distributed in the geopolymer. These observations are characteristic of geopolymers obtained in the literature, in particular for civil engineering applications [51,59]. Foaming agent imparts porosity in the materials while preserving their mechanical characteristics. As the amount of peroxide increases, the connections between the pores increases leading to the formation of open and interconnected pores. This type of structure is also observed by Deng et al. [60,61]. These results show that average pore size increases very significantly with the amount of foaming agent. When foaming agent is applied in amounts larger than the standard applied in the literature (v = 1 ml) [52], a new foam-like structure is formed that is characterized by the formation of bridges and interconnected walls and porous zones. The pores are of variable size and randomly distributed in the volume. These geopolymer materials with macroporous properties are characteristic of alveolar foams [12]. Their mechanical properties (brittleness) are of little interest for civil engineering applications, so they are not studied in the literature. However, these alveolar foams develop porous characteristics that are highly sought after for photoreactor applications [7,62].

Fig. 5 shows pictures obtained for two types of surfactant (CTAB and SDS) at different masses (0.01–0.3 g). The active surfactant acts on the formation of bubbles during the foaming process, allowing the porosity to stabilize. Note that foams produced without surfactants develop closed or very weakly interconnected porosity. The SDS surfactant appears to promote the formation of closed pores whereas CTAB induces the formation of a network of interconnected open pores. As the surfactant concentration increases, it favors the formation of interconnected open cellular-type pores. If the amount of surfactant is too high, we observe the development of walls between the pores which tend to close.

Drying temperature also influences the size and type of porosity (Fig. 6). For a drying temperature of 25 °C, the pores are few in number, with thick walls and few or no connections. A drying temperature of 60 °C induces the formation of cellular-type porosity with geometrically-shaped walls and pores of relatively homogeneous size. At high drying temperatures (80 °C), walls are formed again, thus reducing the number of pores and leading to a large pore-size distribution. During the drying process, the temperature affects the size of the bubbles formed. It is likely that an over-high temperature causes large gas bubbles to form too quickly, which is not conducive to the creation of pores with controlled properties, whereas a drying temperature of 40 °C appears to be suitable.

Tests were also carried out with the replicate method (Fig. 7). In agreement with the literature, the foams developed with a PE matrix have an open and interconnected porosity [45,63]. With the PEM foam, the pores are homogeneously distributed in the form of a reticular structure, whereas with the PEL foam, the formation of walls is more pronounced and the pores are fewer and smaller. Furthermore, PU foam has a heterogeneous structure with a large pore-size distribution. The pores are of different natures (closed and open) and are generally poorly connected and randomly distributed in the volume.

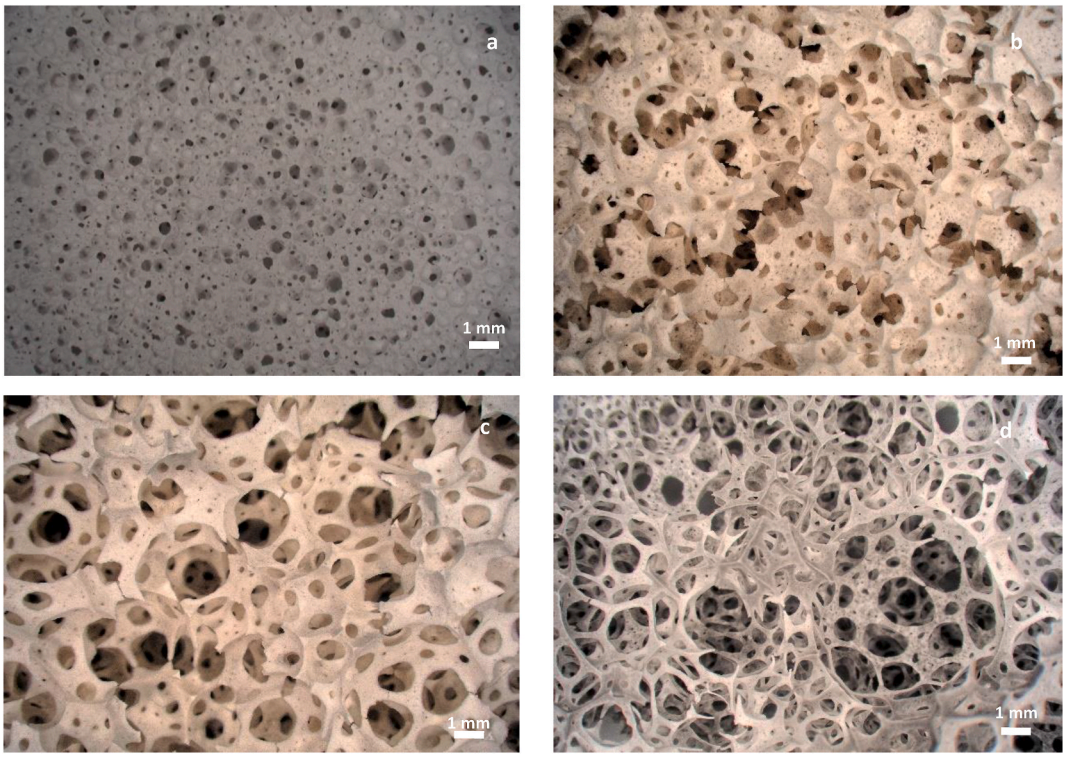

Fig. 4. Photograph -obtained with high-resolution optical microscope-of geopolymer foams elaborated by direct foaming method with different volumes of foaming agent (from a to d): hydrogen peroxide volumes of 0.05, 0.5, 1 and 4 ml (foam 1 t 5 in Table n°1).

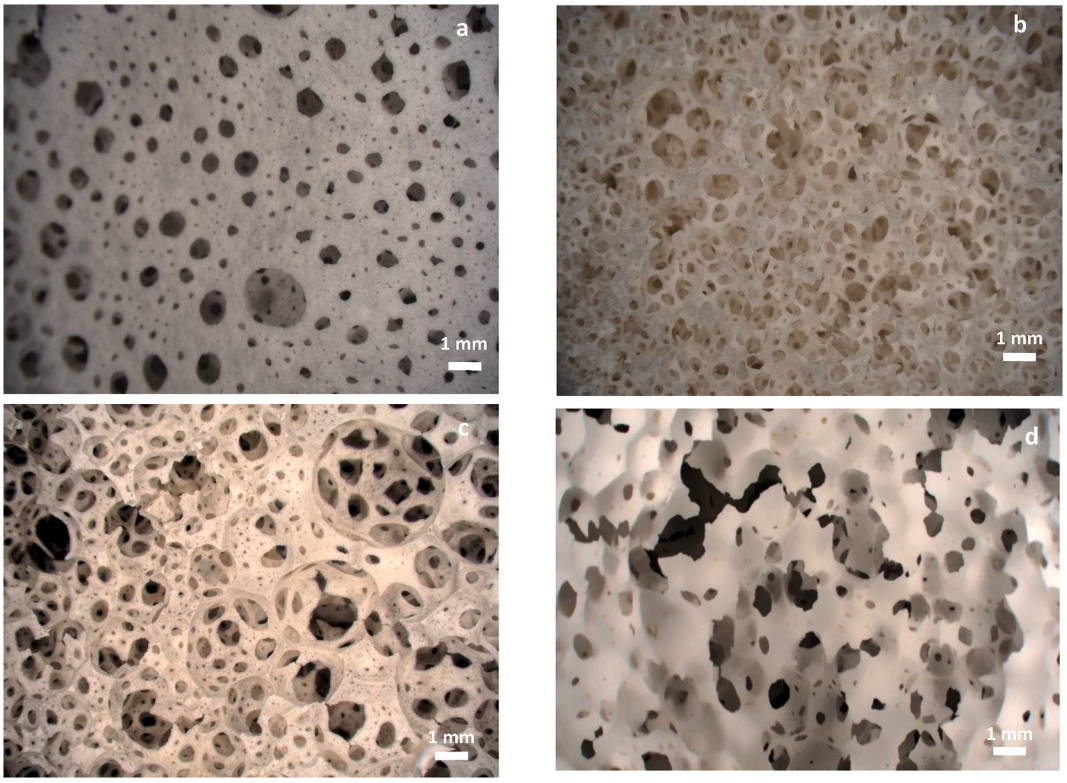

Fig. 5. Photographs -obtained with high-resolution optical microscope-of geopolymer foams elaborated by direct foaming method (foam 8, 10 and 15 in Table n°1) without surfactant (a), with SDS (b), with CTAB (m = 0,1g) (c) and with CTAB (m = 0.3g) (d).

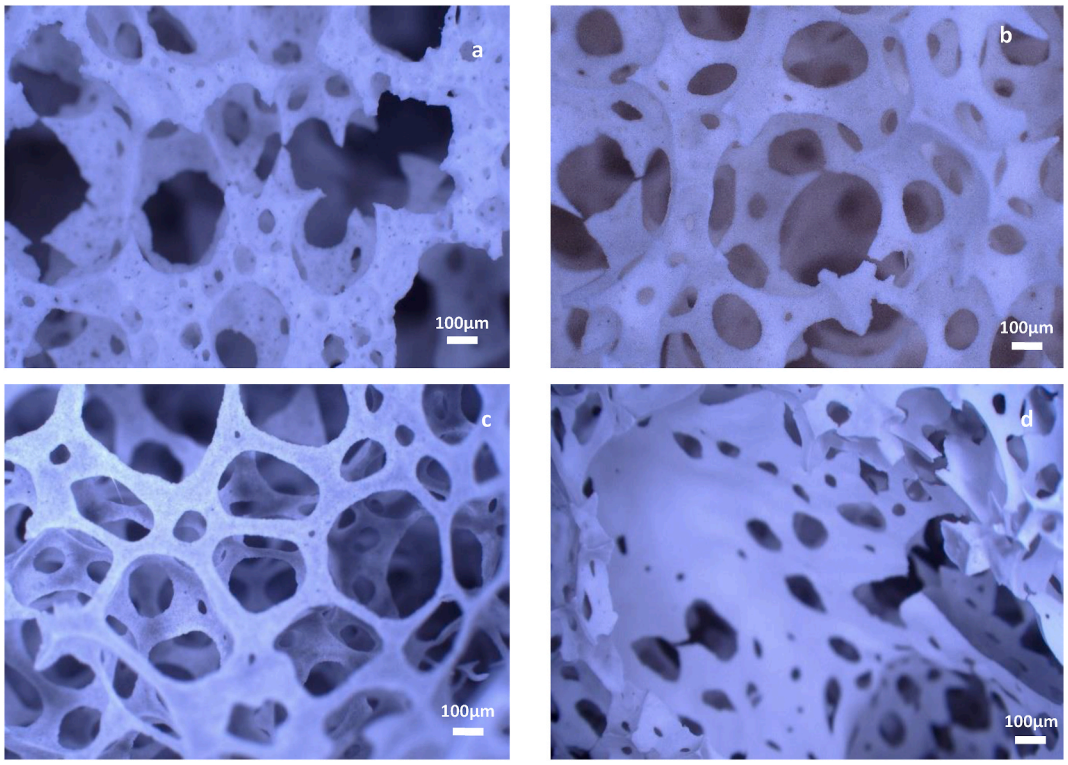

Fig. 6. Photographs -obtained with high-resolution optical microscope-of geopolymer foams elaborated by direct foaming method (reference foam and foams 11 to 13 in Table n°1) dried at different temperature: 25 °C (a), 40 °C (b), 60 °C (c) and 80 °C (d).

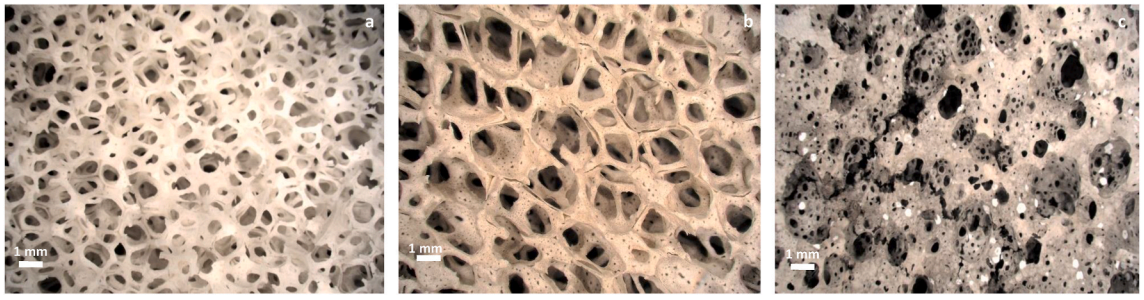

Fig. 7. Photographs -obtained with high-resolution optical microscope-of geopolymer foams elaborated by replica method using different polymeric support: poly ethylene with medium porosity –PEM (a), polyethylene with large porosity –PEG (b) and polyurethane -PU (c).

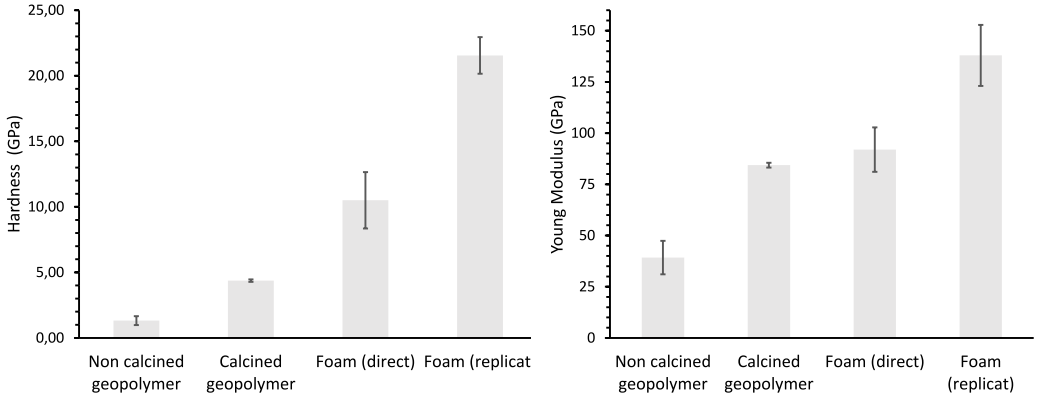

Fig. 8. Mechanical properties of uncalcined and calcined geopolymer and geopolymer foams obtained by direct foaming and replication methods: Hardness (a) and Young's modulus (b).

2.5. Analysis of mechanical properties

Measurements of hardness, which characterizes resistance to plastic deformation, and Young's modulus, which characterizes resistance to elastic deformation, were carried out on four samples: non-calcined geopolymer, calcined geopolymer, geopolymer foam, and geopolymer foam made by the replication method (Fig. 8). The mechanical characteristics of the geopolymer are consistent with results in the literature, with a hardness of 1.3 GPa and a Young's modulus of 39.2 GPa [38,39]. The mechanical properties induced during the inorganic polycondensation process are obtained by drying at room temperature [52, 61]. For this study, the geopolymers were calcined at a temperature of 800 °C for 2h. This heat treatment significantly increases the mechanical characteristics. The hardness increases by a factor of 3 and Young's modulus increases by a factor of 2. This heat treatment does not really make sense for geopolymers intended for civil engineering applications for example, but it appears very promising for improving the mechanical performances of geopolymers intended for photo-conversion. If the same heat treatment is applied to a geopolymer foam elaborated with an active surfactant, Young's modulus remain constant while hardness increases by a factor close to 2. The work of Kovarik et al., shows that the nature of the active surfactants modifies the mechanical properties, which some surfactants can very significantly improve by a factor varying from 1 to 4 [41]. Surfactant concentration seems to play a secondary role [40]. The mechanical properties achieved at the nanoscale on geopolymer foams elaborated by replication are much higher than those of other geopolymers studied. Hardness values reach 22 GPa and Young's modulus reaches 139 GPa. Note that the foaming and heat treatment steps after drying tend to improve the mechanical properties of geopolymers.

2.6. Determination of composition

The XRD spectrum of the geopolymer, shown in Fig. 9, reveals a halo pattern between 15° and 35° (2θ). This result is consistent with what many authors have obtained for this kind of material and is characteristic of an $Al_2O_3.2SiO_2$ kaolin material [64–67]. The main diffraction peaks (square, ■) collected at 2θ are assigned to a sodium alumino silicate compound ($NaAlSiO_4$, Nepheline ICDD-JCPDS card N°75–2933) [56]. A minor crystalline phase could be assigned to an aluminium silicon oxide compound ($Al_2(Al_{2.588}Si_{1.412})O_{9.706}$, ICDD-JCPDS card N°74–8549) characterized by the main diffraction peaks (circle, ●) [68]. Indeed, the Si, O, and Al detected through EDS analysis were consistent with the peaks observed on the X-ray diffractogram, highlighting the presence of kaolinite and quartz.

The mass variation and heatflow curves of the kaolin geopolymer foam sample are presented in Fig. 10. It was found that few changes occurred during the heating process. First, some free water was released during heating until 100 °C. This phenomenon is characterized by an endothermic peak at 100 °C on the heatflow curve and a sample weight loss of around 8 %. Second, another endothermic peak was observed between 450 and 500 °C on heatflow curves, corresponding to the dehydroxylation of kaolinite and the formation of metakaolinite. This result is consistent with previous findings [65,69]. This phenomenon induces only negligible weight loss, as it can be observed on the thermogravimetric signal at this temperature. The thermogravimetric curve goes on to show substantial weight loss between 700 and 800 °C. In this range, the heatflow curve shows an endothermic peak. This phenomenon is not characteristic of the kaolin material., However, this kind of endothermic release was clearly highlighted during the preparation of polymer-derived ceramic foams using polymeric additive through the process [45]. We therefore assume that this phenomenon has to be related to the pyrolytic release of gases from residual organic molecules introduced by the surfactant (CTAB and SDS).

In conclusion, this section on property characterization shows that the various analyses are in line with what is expected in the literature. The geopolymeric foams produced have the signature of the geopolymeric material in terms of both composition and structure. The mechanical properties of the geopolymer foam skeleton are characteristic of a solid material and are suitable for potential applications. The microporous network, in line with the literature, corresponds to that of zeolite materials.

2.7. Results

The aim is to monitor the pore characteristics of geopolymer foams synthesized by the direct foaming method and by the replication method. The photographs taken are used to define the type of porous network developed. This involves determining whether the network is made up of closed, open, reticulated or interconnected pores. A measurement procedure has been developed to define the main porosity characteristics, such as pore size distribution, total pore surface area and overall porosity. Geopolymer foams were studied to assess the influence of the elaboration method and synthesis conditions on porosity characteristics, focusing on the possibility of obtaining a macroporous interconnected cellular network made up of millimetric pores.

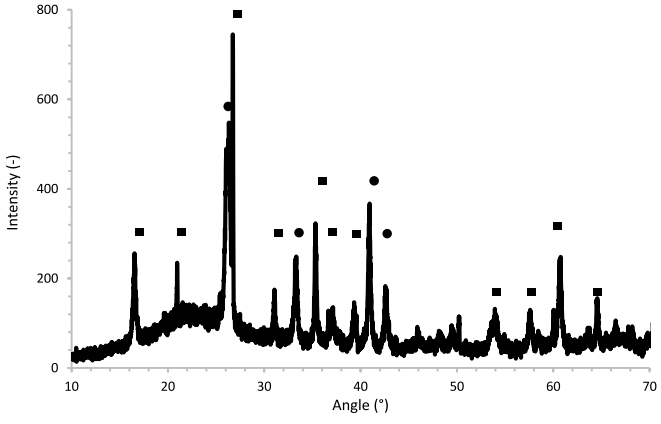

Fig. 9. Diffraction pattern (10–70°) collected for geopolymer foam (reference foam in the table n°1) composed by $NaAlSiO_4$ (■) and $Al_2(Al_{2.588}Si_{1.412})O_{9.706}$ (●).

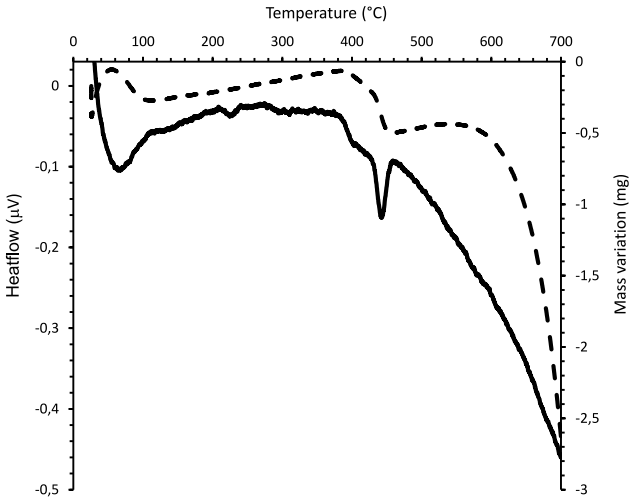

Fig. 10. Results obtained by thermogavimetric analysis of geopolymer foam (reference foam in Table 1): variation in mass (–) and heatflow (–).

2.8. Direct method:optimization of porous characteristics

In the literature, the concentration of foaming agent and surfactant are the two key parameters for modulating the porosity characteristics of geopolymer foams. Here we study the influence of these two parameters over a wide range of conditions. The objective is to define the ranges of operating conditions for the required porosity properties and to be able to modulate them according to the target application. Beforehand, the synthesis operating conditions, i.e. drying temperature and type of surfactant, were studied. The aim is to select and set the conditions for the study of key parameters such as foaming agent and surfactant concentration.

2.8.1. Determination of geopolymer foam synthesis conditions

Experiments were conducted to define the conditions required to develop geopolymer foams with controlled pore properties and reticular form. The conditions tested were inspired by the literature but over a wider range of values [42,52,57,61,70]. A wide variety of surfactants have been studied in the literature [52,71,72], and it appears that CTAB and SDS are the surfactants most commonly used to obtain homogeneous pore structures by allowing bubble stabilization during foaming. Fig. 11 plots the pore fractions of three pore classes representative of the pore distribution in the volume of the foams for both types of surfactants. For CTAB, the pores are homogeneously distributed over the 0–1000 μm (small pore size class) and 1000–2000 μm (medium pore size class) size classes, while pores larger than 2000 μm (large pore size class) are almost non-existent (fraction <0.05). This surfactant promotes the formation of homogeneous pore sizes over a range up to 2000 μm, playing its role as a stabilizer of bubble formation during the foaming process [52,72]. SDS appears to promote the creation of smaller pore sizes. Smaller pore sizes represent a porosity fraction of 0.70 while medium and large pore sizes represent a porosity fraction less than 0.2 each. These results, in agreement with the microscopic observations, show that CTAB allows the creation of pores over a wider size range, which is quite different from what is observed in the literature [71–73]. The authors show that the pore diameters formed are well below 500 μm, whereas Fig. 11 shows that the geopolymer foams developed here form larger pore sizes. Klima et al., implemented a foaming agent-to-aluminosilicate ratio of 0.025 [72]. Our study was based, among others, on the work of Sanson Samsom [70] where foaming agent-to-aluminosilicate ratio varies from 0.01 to 0.8. A larger quantity of foaming agent induces the formation of greater porosity and larger-diameter pores. This route was chosen as the best way to structure a macroporous cellular-type foam. Klima et al., also indicate that SDS appears to promote the creation of an open porosity whereas CTAB induces the formation of closed porosity [72]. On other hand, our results show that at equal amounts, the type of surfactant has little influence on the type of porosity obtained (open or closed), whereas a high surfactant concentration (CTAB) allows to create open pores.

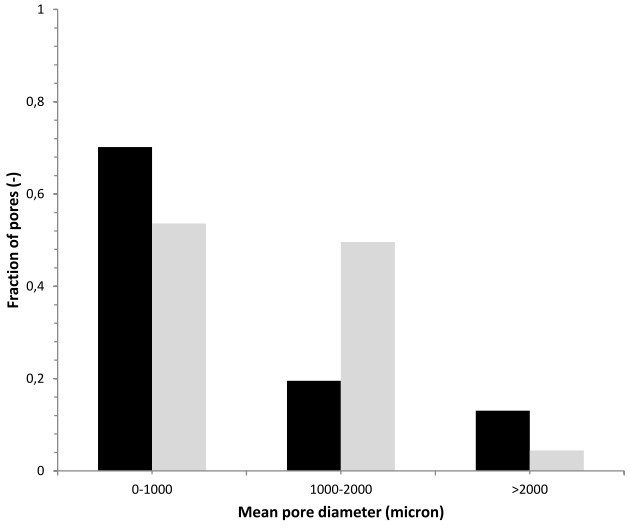

Fig. 11. Variation in pore volumic fraction, obtained by image processing, according to three pore size classes. Results obtained on geopolymer foams synthetized by the direct foaming method (foams 14 and 15 in Table 1) with two surfactants, SDS (black) and CTAB (grey).

Drying temperature also plays a role in the foaming process [22]. Geopolymer foams were synthesized and dried during the foaming process at different temperatures ranging from 25 to 80 °C. The curve plotting variation in porosity as a function of temperature (Fig. 12a) shows a plateau at a temperature range of 40°C-60 °C, at which the porosity by volume reaches 0.8. If an over-high temperature is applied, porosity decreases. Likewise, a low drying temperature does not appear to promote the development of porosity.

The results reported in Fig. 12b show that the temperature modifies the pore-size distribution very significantly and in different ways for different pore size classes. Small and medium-size pores fraction show an optimum for drying temperatures of 40 and 60 °C, respectively, whereas large-size pores are formed predominantly when temperatures become higher than 60 °C. This result indicates that the temperature favors the growth of bubbles by expanding the peroxide bubbles contained in the geopolymer during the foaming process. Our microscopy observations indicate that a high temperature induces the formation of a heterogeneous pore network and a destructured foam. These temperature conditions do not lead to a uniform porous structure with controlled characteristics. Note that at 25 °C, the fractions of small and medium-size pores are very similar, whereas at 80 °C, all three size classes (small, medium, and large) are in similar fractions.

2.8.2I. nfluence of the foaming agent

The standard conditions of use of a foaming agent make it possible to obtain geopolymer foams that develop high porosity while maintaining their mechanical properties [22, 23,31,32]. The pore size distribution obtained is large and covers mainly the nanoporous and microporous range. In order to significantly increase the porosity, geopolymers have been elaborated with a ratio of foaming agent to alkaline solution ranging from 0.1 to 10 times the conditions usually applied [43,51,52]. For this purpose, we used the reference geopolymer elaboration procedure by modulating the peroxide volume from 0.05 to 4 ml.

First we looked at the effect of foaming agent concentration on the surface and volume porosity fraction. Both surface and volume porosity increase very significantly as a function of foaming agent (Fig. 13a). The porosity fraction is less than 0.1 for peroxide contents below 0.2 ml but can reach more than 0.8 for high peroxide contents (v = 4 ml). These results, in agreement with the literature, show that modifying the peroxide content makes it possible to dramatically modulate geopolymer porosity and make the pore structure evolve from closed pores to a reticular structure (Fig. 4). In the review by Shen [22], geopolymers made from mortars, cements and pastes develop porosities ranging from 0.1 to 0.5 [74,75]. The geopolymer foams developed by Nguyen have a porous reticular structure with a porosity range of 0.3 to over 0.85 [76].

The evolution of the pore-size distribution depends on the foaming agent concentration [32]. As illustrated by our results (Fig. 13b), the changes in pore size are particularly significant at low peroxide concentrations. For volumes below 1 ml, there is a very significant increase in the medium- and large-size pore classes, apparently at the expense of the small-size pores. Small amounts of peroxide favor the formation of small bubbles during the foaming process which induce the preferential creation of small pores [22,43,77]. At higher than 1 ml of peroxide, the pore class composition seems to stabilize with pore fractions below 0.2 for large pores, close to 0.3 for medium-size pores, and around 0.5 for small pores. Note that small pore sizes tend to decrease progressively with the amount of foaming agent in favor of large pore sizes [32].

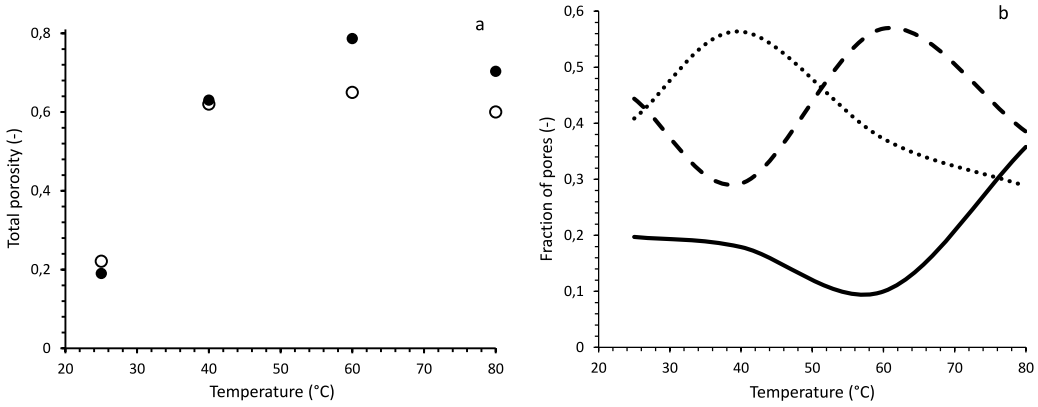

Fig. 12. (a) Variation of the pore fraction of geopolymer foams (reference foam and foams 11 to 13 in the table n°1), obtained by image processing, as a function of drying temperature for three particle size classes; 0–1000 (dotted line), 1000–2000 (dash line) and greater than 2000 μm pore diameter (line). (b) Variation in the volume (●) and surface (○) porosity of geopolymer foams as a function of drying temperature.

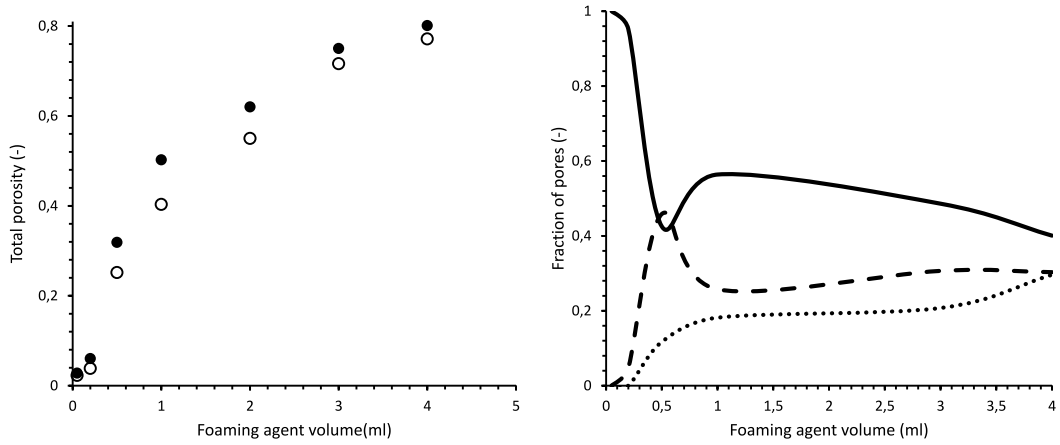

Fig. 13. (a) Variation of the pore fraction of geopolymer foams (foams 1 to 5 in the table n°1), obtained by image processing, as a function of foaming agent volume for three particle size classes; 0–1000 (dotted line), 1000–2000 (dash line) and greater than 2000 μm pore diameter (line). (b) Variation in the volume (●) and surface (○) porosity of geopolymer foams as a function of foaming agent volume.

shows that pore size and open porosity increase significantly with amount of peroxide, but at the expense of the stability of the reaction and homogeneity of the pore size distribution. A large quantity of foaming agent (V > 2 ml) allow pore sizes greater than 2 mm in diameter to be obtained with a maximum porosity of less than 0.6. Our results show that it is possible to achieve higher porosity when applying peroxide volumes greater than 2 ml. Note that generally, the geopolymer foams obtained have porosities lower than 0.6 with mostly micrometric-size pores [31,22], and that surfactants are added to increase the porosity [23]. Replication and air injection methods are applied to obtain open porosities with millimeter-size pores [28,76].

2.8.3. *Influence of the surfactant*

Surfactants are used to stabilize the bubbles during the foaming process and facilitate the formation of the pore network within the geopolymer [43]. To evaluate the effect of the amount of surfactant on porosity (pore size and pore volume), geopolymer foams were developed using amounts of surfactant ranging from 0.01 to 0.3 g of CTAB. This corresponds to surfactant-to-alkaline solution ratios ranging from 0.002 to 0.06, which cover a large panel of conditions compared to the literature [42,43]. The variation of the surface and volume porosity fractions (Fig. 14a) shows an optimum at the reference conditions given in the literature. When the amount of CTAB is insufficient, the pore network is reduced to a value below 0.2, while it reaches 0.7 for a volume of 0.05 of CTAB. Then, the porosity fraction gradually decreases with the amount of CTAB. As suggested by Kaddami [70,73], some surfactants do not mix well with the Kaolin matrix during synthesis. It is also the case when an excess of surfactants is added, which leads to the modification of the rheological behavior of the geopolymer or to the destabilization of bubbles during the foaming process. Other works seem to indicate that the pore network including open and closed porosity increases and then tends to stabilize for a certain amount of surfactant [78], or that the presence of surfactant facilitates the formation of open porosity. In this study, the variation of the porosity as a function of CTAB shows an optimum that corresponds to the transition from geopolymer foams consisting of closed pores to an alveolar structure (Fig. 5). After the optimum, porosity decreases significantly, in line with our SEM observations. Indeed, as surfactant levels rise, the alveolar structure tends to close and form walls. These observations suggest that an optimum surfactant level leads to the formation of a geopolymer foam with a reticulated alveolar structure and high porosity.

A closer analysis of the influence of CTAB on the pore-size distribution finds that the pore size classes do not evolve linearly. For high amounts of CTAB, the three pore size classes are represented almost equally. In this area, the amount of CTAB has little influence on the pore size distribution, which does not change significantly. On the other hand, as illustrated by our observations (Figs. 4 and 5), the pore network evolves from a closed pore structure to an interconnected reticular

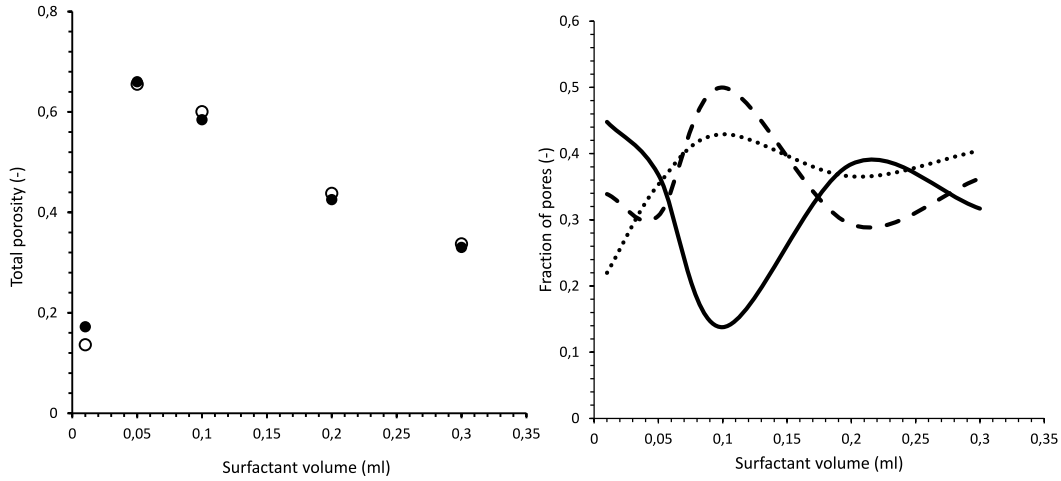

Fig. 14. (a) Variation of the pore fraction of geopolymer foams (reference foam and foams 6 to 10 in the table n°1), obtained by image processing, as a function of surfactant volume according to three particle size classes; 0–1000 (dotted line), 1000–2000 (dash line) and greater than 2000 μm pore diameter (line). (b) Variation in the volume (●) and surface (○) porosity of geopolymer foams as a function of surfactant agent volume.

structure. In this situation, CTAB induces the formation of an interconnected pore network at the expense of total-volume porosity. The reference conditions are very favorable to the formation of small and medium-sized pores, preferentially consisting of closed or partially connected pores, which account for almost 90 % of the porosity, with only a negligible amount of large pores.

It appears from the literature that microporosity and mesoporosity can be modulated using the type and concentration of surfactant [70, 79]. Whereas small bubbles are slow to produce and ripen fast, large bubbles (D > 1 mm) do not undergo ripening. Therefore, the ultra-macroporosity is mainly conditioned by the size of the bubbles formed during foaming and the presence of surfactant which stabilizes the large bubbles. CTAB at v = 0.1 g thus helps to stabilize small bubbles and appears to limit the formation of larger bubbles. When the quantity of CTAB is low, it tends to preferentially stabilize larger bubble sizes. It can be assumed that the surfactant concentration is below the critical micellar concentration and that the surfactant micelles cannot play their role [70]. This situation is particularly unfavorable for small bubbles, which due to their higher specific surface area require more surfactant to cover their surface with micelles. When the quantity of surfactant is high, it acts in an undifferentiated way on all the bubbles formed, which leads to an even distribution over the three pore-size classes (Fig. 14). Note that by adjusting the surfactant-to-alkaline solution ratio, it is possible to modulate the properties of the pore network, such as the pore size distribution and the pore volume [70,77,79,80,20].

2.9. Geopolymer foam via the replication method

The replication technique leads to the use of cellular geopolymer foams that develop an ultra-macroporous network with controlled porosity [81,82]. Choosing the right support allows to impart controlled porous characteristics to the geopolymer foams [28]. Here, three types of polymeric foams were selected as support, i.e. one polyurethane sponge made up of open and closed cells with a large pore distribution, and two cellular-type polyethylene (PE) foams of differing cell size. The porosities obtained with the two PE foams reached 0.85 and 0.9, respectively, with the PEM and PEL media. The porous structure of the foams made with PE media is reticulated, thus forming a network of interconnected pores, as the structure of the PE media consists of well-defined cells and membrane. In the literature, geopolymer foams generally form networks of interconnected pores with porosities in the range 0.7–0.9 [28]. Some works show that it is possible to achieve porosities above 0.9 [45]. Geopolymer foams obtained from a PU sponge give a porosity of 0.65. The PU sponge support, consisting of partially interconnected closed and open pores, leads to the formation of a less organized structure with a large pore-size distribution.

Fig. 15 plots the pore-size distribution in three size classes for the three geopolymer foams developed by replication. The geopolymer foams obtained with a PEM support, consisting of small pore sizes fraction of 0.8 (<1 mm), do not have any pores >2 mm. The pore size distribution is due to the initial structure of the PEM support with monodispersed cells. The pore size distribution of the foams made from PEL supports is homogeneously distributed over the small and medium pore-size classes, while the large pore sizes represent less than 0.1 of the pore fraction. The foams made with PU stand out by developing a porosity that is homogeneously distributed over the three pore classes. The majority of the foams developed by direct foaming have sub-millimeter pore-size distributions [83,84], whereas those developed via replication show a greater diversity of pore networks [22]. Although it is possible to impart millimeter-size porosities via the replication technique [22,45], a large proportion of the foams produced develop sub-millimeter-size pore networks that depend on the structural characteristics of the replicate [28]. In this study, the replicates were

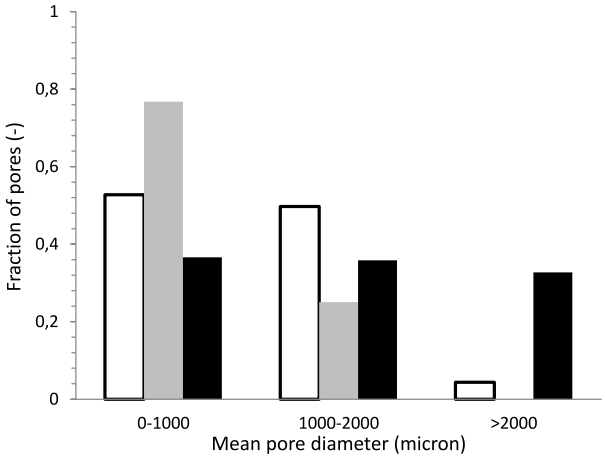

Fig. 15. Variation in the pore fraction -obtained by image processing-of geopolymer foams elaborated with replica method by using three polymeric supports, PU (black), PEM (grey) and PEG (white), according to three particle size classes.

selected in such a way as to obtain a macroporous network consisting mainly of millimeter-sized pores. The structure of the PEM and PEL geopolymer foams is reticulated. The properties of the resulting foams correspond to ultra-macroporous structures characterized by an interconnected network of pores. These geopolymer foams, which are easy to process and offer modular pore characteristics by adjusting the structure of the replicate, make good candidates for many applications. On the other hand, the foams obtained via the PU carrier are made up of a variety of pores ranging from closed, open, and partially-connected pores. When the processing procedure is appropriately adapted, the replication technique can reproduce the porous characteristics of the support media quite accurately.

3. Discussion

The experiments were carried out to cover a wide range of operating conditions, with the aim of modulating the porosity characteristics of geopolymer foams. Ultimately, the aim is to develop geopolymer foams that meet the constraints imposed by use of the solar resource. For a solar photocatalysis application, if we refer to the high-performance macroporous photocatalytic materials developed in the literature, the desired characteristics are oriented towards interconnected alveolar structures with variable porosities depending on the photoreactor configuration [7,9,62]. Indeed, the geometries and thicknesses of the material vary depending on the reactor configuration. For example, for a flat reactor [85], the material integrated into the photoreactor must be thin (1–2 cm), which implies a cellular foam with low porosity or made up of small-diameter (i.e. around 1 mm) pores to capture all the solar radiation over the given thickness. For a tubular geometry, greater thicknesses can be envisaged to ensure that more incident radiation is captured, which makes foams with high porosities or with larger pore diameters (a few millimeters) more suitable [9,86,87]. In this context, the results obtained here are important as they show that it is possible to obtain a wide panel of geopolymer foams that differ in terms of their structure, porosity level, and pore size distribution according to the three classes selected. Depending on the process conditions, the foams present matrices with partially or totally closed pores, matrices with totally or partially connected open pores, and interconnected alveolar structures.

In line with what is described in the literature, a foam elaborated with no or very little surfactant leads to the formation of a low porosity exclusively made up of closed pores, especially with SDS compared to CTAB. This may be relevant for a civil engineering application to preserve mechanical properties, but is unsuitable for a solar photo-oxidation application. The influence of surfactant quantity is crucial. Maximum porosity is obtained for surfactant-to-alkaline solution ratios of 0.01–0.02, in line with the literature [41,88]. The transition from a closed-pore structure to an alveolar structure occurs at a surfactant-to-alkaline solution ratio of 0.02. As surfactant ratio increases, porosity decreases. The meshes and walls of the alveolar structure also tend to thicken. In these conditions, pore-size distribution is equally distributed over the three pore-diameter classes (Fig. 14). Thus, for the intended application, a surfactant-to-alkaline solution ratio of 0.02 seems to be a good compromise for obtaining an interconnected alveolar foam, even if it is possible to modulate the mesh/pore characteristics by playing on this ratio.

Results on the effect of the foaming agent, which was studied over a wide range of values, confirm what has been established in the literature [22,31,88]. Logically, the greater the amount of foaming agent, the greater the increase in porosity. A threshold foaming agent-to-alkaline solution ratio of 0.8, beyond which the foam's mechanical properties become too weak, has been observed. Although drying and calcination improve the mechanical properties (hardness and Young's modulus) of the foam, our conditions do not allow the use of foams produced with higher ratios. This is an avenue to be explored with a view to developing cellular foams with higher porosities. Note that there is a minimum amount of foaming agent required (foaming agent-to-alkaline solution ratio of 0.1) to move from a closed-pore matrix to a cellular structure. Beyond this threshold, the alveolar structure evolves towards the formation of finer walls and meshes, while the pore-size distribution remains almost unchanged. It is therefore possible to modulate foam properties both in terms of total porosity over a range from 0.4 to 0.8 (Fig. 13) and the characteristics of the alveolar structure (meshes and walls) (Fig. 4), while preserving a substantially similar pore-size distribution. Note, too, that structures with a high pore size distribution induce radiation scattering phenomena within the photoreactor, which is a desirable feature for these applications [53,62].

Drying temperature plays a key role in controlling the porous properties of geopolymer foams and has a strong influence on pore size distribution, structure type, and total porosity. First, drying temperatures above 40 °C produce the highest porosities (0.6–0.8). However, only the 40°C-60 °C temperature range leads to the formation of an interconnected alveolar structure. Outside this range, geopolymer foams tend to produce closed pores (T = 25 °C) or an alveolar structure consisting of pores with very large walls and meshes that tend to close (Fig. 6). Pore-size distribution varies considerably is from one drying condition to another. If we focus our attention on the 40°C-60 °C range, which enables the formation of alveolar structures, we note that these two conditions enable us to obtain two complementary structures (Fig. 12). A drying temperature of 40 °C favors the formation of small-diameter pores is (fraction>0.55) at the expense of other pore diameter classes, whereas a temperature of 60 °C leads to predominantly medium-size-diameter pores. This finding is valuable for adapting the characteristics of foams to the configuration of a photoreactor, as it offers the possibility of modulating the pore size distribution without changing the pore characteristics.

We also investigated the possibility of creating geopolymer foams using the replication method. Our results show that it is possible to reproduce complex geopolymer structures fairly faithfully to replicas, and thus to offer a wide range of porous structures based on the characteristics of existing polymeric foams. PU replicas enabled the development of geopolymer foams that were fairly chaotic in terms of structure but that had a homogeneous pore size distribution. PE replicas, on the other hand, enabled alveolar structures to be obtained while modulating pore size distribution. The value of this approach lies in the possibility of elaborating foams with repeatable and well-defined characteristics in order to carry out comparative studies, for example, on the influence of porous properties on radiative transfer, flow conditions, or photo-reactive capacities [2,53,62]. This method seems to offer the means to modulate and control the porous characteristics of the geopolymeric foams produced. It confers the expected properties, i.e. a macroporous (porosity >0.85) interconnected honeycomb network made up of millimetric pores.

4. Conclusion

The aim of this study was to optimize an experimental methodology for developing macroporous geopolymer foams with an interconnected honeycomb structure. The target criteria were to obtain a honeycomb structure, a macroporous network of millimetric pores and a high porosity greater than 0.75, which is the threshold for the transition from closed to open porosity. The materials were first characterized to verify that their structural properties, composition and mechanical properties were as expected. Our approach consisted in using the two main elaboration methods and studying the influence of the main elaboration parameters, i.e. (1) for the direct foaming method, the concentration of foaming agent, surfactant and drying temperature were studied, and (2) for the replication method, the type and porosity of the replica were considered.

The replication method was used to obtain foams with the desired porous properties. As expected, with this method, it was possible to obtain macroporous cellular geopolymer foams made up of

interconnected millimetric pores. The characteristics of the geopolymer foams obtained are similar to those of the replicas. On the other hand, PU replicas fail to control the porous characteristics of geopolymer foams, resulting in a disordered structure with a high pore size distribution.

The direct foaming method has produced a wide range of foams distinguished by their porous properties. Under certain conditions, and in particular when the foaming agent or surfactant is insufficient in quantity, the foams obtained have low porosity structures, consisting of closed pores or partially connected pores. The drying temperature tends to greatly increase porosity and promote the formation of a honeycomb network. Once the amount of surfactant and drying temperature have been optimized, the key operating parameter for modulating pore characteristics is the foaming agent. The selected foaming agent significantly increases the porosity of geopolymer foams while preserving relatively similar pore size distributions. By optimizing the synthesis conditions in adjusting the amount of foaming agent, it has been possible to elaborate macroporous geopolymer foams (porosity 0.75–0.89), with a honeycomb structure made up of interconnected millimetric pores.

In perspective, this study has demonstrated the feasibility of producing macroporous cellular geopolymer foams. By adjusting the conditions of elaboration, it is possible to modulate the porous characteristics. Once functionalized with a photocatalytic film, these geopolymer foams are intended for integration into a solar photoreactor. These materials are of great interest for improving the ability of photoreactors to make optimum use of solar resources.

CRediT authorship contribution statement

S. Benkhirat: Writing – original draft, Formal analysis, Data curation. **G. Plantard:** Supervision, Funding acquisition. **E. Ribeiro:** Methodology. **H. Glenat:** Formal analysis, Data curation. **Y. Gorand:** Formal analysis, Data curation. **K. Nouneh:** Supervision, Methodology, Investigation, Funding acquisition.

Declaration of competing interest

The authors declare that they have no known competing financial interests or personal relationships that could have appeared to influence the work reported in this paper.

Data availability

Data will be made available on request.

Acknowledgements

This work received regional sponsorships “Projet Recherche et Société Région Occitanie” AQUIREUSE (N°20019602) as well as “Programme Hubert Curie-PHC Toubkal” (n°47219QH). We would also like to thank Denis Chaumont for enabling us to carry out DRX and porosimetry analyses in his laboratory.

References

[1] B. Degrenne, J. Pruvost, G. Christophe, J.F. Cornet, G. Cogne, J. Legrand, Investigation of the combined effects of acetate and photobioreactor illuminated fraction in the induction of anoxia for hydrogen production by Chlamydomonasreinhardti, Int. J. Hydrogen Energy 35 (19) (2010) 10741–10749.
[2] G. Plantard, B. Reoyo, A. Sellier, S. Khaska, C. Le Gall Lasalle, K. Weiss, V. Goetz, Performances of a pool-type photoreactor operating in continuous mode under solar irradiation for the treatment of pollutants contained in wastewater, Journal of Water and Process Engineering (2023).
[3] S. Malato, P. Fernandez-Ibanez, M.I. Maldonado, J. Blanco, W. Gernjak, Decontamination and disinfection of water by solar photocatalysis: recent overview and trends, Catal. Today 147 (2009) 1–59.
[4] J.B. Galvez, S. Malato, Solar Detoxification, united Nations Educational, Scientific and Cultural Organization, 2003.
[5] C. Supplis, Modélisation et étude expérimentale de la production solaire de dihydrogène, Thesis of Clermont-ferrand University, 2020.
[6] G. Flamant, B. Grange, J. Wheeldon, F. Siros, F. Valentin, F. Bataille, F. Zhang, J. Baeyen, Opportunities and challenges in using particle circulation loops for concentrated solar power applications, Prog. Energy Combust. Sci. 94 (2023) 101056.
[7] G. Plantard, V. Goetz, Correlations between optical, specific surface and photocatalytic properties of media integrated in a photo-reactor, Chemical of Engineering Journal 252 (2014) 194–201.
[8] G. Plantard, Du matériau divisé au photo-réacteur solaire, in: Habilitation à Diriger les REcherches, University of Perpignan, 2014.
[9] I. Ochuma, O. Osibo, R. Fishwick, S. Pollington, A. Wagland, J. Wood, J. Winterbottom, Three-phase photocatalysis using suspended titania and titania supported on a reticulated foam monolith for water purification, Catal. Today 128 (2007) 100–107.
[10] G. Plesh, M. Gorbar, U. Vogt, J. Jesenak, M. Vargova, Reticulated macroporous ceramic foam supported TiO_2 for photocatalytic applications, Mater. Lett. 63 (2009) 461–463.
[11] A. Serpone, Relative photonic efficiencies and quantum yields in heterogeous photocatalysis, J. Photochem. Photobiol. Chem. 104 (1997) 1–12.
[12] F. Topin, Habilitation à Dirigés la recherche, université de Provence, Phénomènes de transport en milieux poreux : matériaux cellulaires à forte perméabilité - morphologie (2006). ébullition et couplages.
[13] T. Van Gerven, G. Mul, J. Moulijn, A. Stabkiewicz, A review of intensification of photocatalytic processes, Chem. Eng. Pross. 46 (2007) 781–789.
[14] M. Motegh, M. Cen, P. Appel, J. Ommen, M. Kreutzer, Photocatalytic-reactor efficiencies and simplified expressions to assess their relevance in kinetic experiments, Chem. Eng. J. 207–208 (2012) 607–615.
[15] Y. Liu, C. Shi, Z. Zhang, N. Li, An overview on the reuse of waste glasses in alkali-activated materials, Resour. Conserv. Recycl. 144 (2019) 297–309.
[16] C. Shi, A.F. Jiménez, A. Palomo, New cements for the 21st century: the pursuit of an alternative to Portland cement, Cem. Concr. Res. 41 (2011) 750–763.
[17] H.R. Gavali, A. Bras, P. Daria, R. Ralegaonkar, Development of sustainable alkali-activated bricks using industrial wastes, Constr. Build. Mater. 215 (2019) 180–191, https://doi.org/10.1016/j.conbuildmat.2019.04.152.
[18] A. Palomo, M. Grutzeck, M. Blanco, Alkali-activated fly ashes: a cement for the future, Cem. Concr. Res. 29 (1999) 1323–1329, https://doi.org/10.1016/S0008-8846(98)00243-00249.
[19] J. Davidovits, Geopolymeric reactions in archaeological cements and in modern blended cements, Concr. Int. 9 (1987) 23–29.
[20] C. Baia, P. Colomboa, Processing, properties and applications of highly porous geopolymers: a Review, Ceram. Int. 44 (2018) 16103–16118.
[21] J. Bell, W. Kriven, Preparation of ceramic foams from metakaolin-based geopolymer gels, Ceram. Eng. Sci. Proc. (2009) 97–112.
[22] Y. Chen, S. Ruan, Q. Zeng, Y. Liu, M. Zhang, Y. Tian, D. Yan, Pore structure of geopolymer materials and its correlations to engineering properties: a review, Construct. Build. Mater. 328 (2022) 127064.
[23] C. Baia, P. Colomboa, High-porosity geopolymer membrane supports by peroxide route with the addition of egg white as surfactant, Ceram. Int. 43 (2017) 2267–2273.
[24] X. Zhang, C. Bai, Y. Qiao, X. Wang, D. Jia, H. Li, P. Colombo, Porous geopolymer composites:a review, Composites 150 (2021) 106629.
[25] C. Bai, B. Li, C. ma, X. Li, X. Wang, B. Wnag, K. Yang, P. Colombo, Open cell cordierite-based foams from eco-friendly geopolymer precursors via replica method, Ceram. Int. 50 (2024) 15340.
[26] A.R. Studart, U.T. Gonzenbach, E. Tervoort, L.J. Gauckler, Processing routes to macroporous ceramics: a review, J. Am. Ceram. Soc. 89 (2006) 1771–1789.
[27] S. Bi, M. Liu, J. Shen, X. Hu, L. Zhang, Ultrahigh self-sensing performance of geopolymer nanocomposites via unique interface engineering, ACS Appl. Mater. Interfaces 9 (14) (2017).
[28] T. Kovárík, T. Krenek, D. Rieger, M. Pola, SvobodaM. JanRíha, J. Beneš, J. Kadlec, Synthesis of open-cell ceramic foam derived from geopolymer precursor via replica technique, Mater. Lett. 209 (2017) 497–500.
[29] X. Wen, G. Rao, L. Wan, S. Wang, K. Lai, G. Yang, F. Ai, Factors affecting the property of open-cell fly ash-based porous geopolymer via replica method, Adv. Cement Res. (2024) 1–25.
[30] E. Fiume, S. Ciavattini, E. Verné, F. Baino, Foam replica method in the manufacturing of bioactive glass scaffolds: out-of-date technology or still underexploited potential? Materials ceramic 14 (2021) 2795.
[31] V. Ducman, L. Korat, Characterization of geopolymer fly-ash based foams obtained with the addition of Al powder or H2O2 as foaming agents, Mater. Char. 113 (2016) 207–213.
[32] A. Hajimohammadi, T. Ngoa, P. Mendisa, T. Nguyena, A. Kashania, J. Deventer, Pore characteristics in one-part mix geopolymers foamed by H2O2: the impact of mix design, Mater. Des. 130 (2017) 381–391.
[33] A. Hajimohammadi, J.L. Provis, J.L. van Deventer, The effect of silica availability on the mechanism of geopolymerisation, Cem. Concr. Res. 41 (3) (2011) 210–216.
[34] P. Palmero, A. Formia, P. Antonaci, S. Brini, J. Tulliani, Geopolymer technology for application-oriented dense and lightened materials. Elaboration and characterization, Ceram. Int. 41 (2015) 12967–12979.
[35] R. Novais, L. Buruberri, G. Ascensão, M. Seabra, L. Labrincha, Porous biomass fly ash-based geopolymers with tailored thermal conductivity, J. Clean. Prod. 119 (2016) 99–107.
[36] H.A. Abdel-Gawwad, M.S. Mohammed, S.E. Zakey, Preparation, performance, and stability of alkali-activated-concrete waste-lead- bearing sludge composites, J. Clean. Prod. 259 (2020) 120924.

[37] S. Hanjitsuwan, S. Hunptratub, P. Thongbai, S. Maensiri, V. Sata, P. Chindaprasirt, Effects of NaOH concentrations on physical and electrical properties of high calcium fly ash geopolymer paste, Cem. Concr. Compos. 45 (2014) 9–14.

[38] M. Zhang, H. Xu, A. Zeze, J. Zhang, Metakaolin-based geopolymer composites modified by epoxy resin and silane: mechanical properties and organic-inorganic interaction mechanism, Appl. Clay Sci. 232 (2023) 106767.

[39] P.G. Allison, C.A. Weiss, R.D. Moser, A.J. Diaz, O.G. Rivera, S.S. Holton, Nanoindentation and SEM/EDX characterization of the geopolymerto-steel interfacial transition zone for a reactive porcelain enamel coating, Composites, Part B 78 (2015) 131e137.

[40] G. Ouyang, L. Wu, C. Ye, J. Wang, T. Dong, Effect of silane coupling agent on the rheological and mechanical properties of alkali-activated ultrafine metakaolin based geopolymers, Construct. Build. Mater. 290 (2021) 123223.

[41] T. Kovářík, J. Hájek, M. Pola, D. Rieger, M. Svoboda, J. Beneš, P. Šutta, K. Deshmukh, V. Jandová, Cellular ceramic foam derived from potassium-based geopolymer composite: thermal, mechanical and structural properties, Mater. Des. 198 (2021) 109355.

[42] S. Petlitckaia, Synthèse de mousses géopolymères à porosité contrôlée :application à la décontamination nucléaire, thèse de l'université Montpellier, 2018.

[43] J. Henon, Elaboration de matériaux poreux géopolymères à porosité multi-échelle et contrôlée, Thèse Université de Limoges, 2012.

[44] L. Tian, W. Zhi, Z. Taotao, H. Yunfei, H. Fangmei, Preparation and properties of magnesium phosphate cement foam concrete with H2O2 as foaming agent, Construct. Build. Mater. 205 (2019) 566–573.

[45] K. Schelm, E. Morales, M. Schefer, Mechanical and surface-chemical properties of polymer derived ceramic replica foams, Materials (2019).

[46] G. Görhan, G. Kürklü, The influence of the NaOH solution on the properties of the fly ash-based geopolymer mortar cured at different temperatures, Composite Part B 58 (2014), 371–7.

[47] J. Henon, A. Alzina, J. Absi, D.S. Smith, S. Rossignol, Potassium geopolymer foams made with silica fume pore forming agent for thermal insulation, J. Porous Mater. 20 (2013) 37–46.

[48] S. Ahmer, A. Shamsuddin, R. Rashid, Ekmi R. Nurul, Z. Muhammad, M. Zakaria, L. Aaron, Fly ash based geopolymer for the adsorption of anionic surfactant from aqueous solution, J. Clean. Prod. (2019).

[49] P. Rovnaník, Effect of curing temperature on the development of hard structure of metakaolin-based geopolymer, Constr Build Mater 24 (7) (2010), 1176–118.

[50] R. Cioffi, L. Maffucci, L. Santoro, Optimization of geopolymer synthesis by calcination and polycondensation of a kaolinitic residue 40 (1) (2003) 27–38.

[51] R. Singla, M. Senna, T. Mishra, T.C. Alex, S. Kumar, High strength metakaolin/epoxy hybrid geopolymers: synthesis, characterization and mechanical properties, Appl. Clay Sci. 221 (2022) 106459.

[52] G. Samson, Synthèse et propriétés des mousses minerals, 2015 thesis University of Limoges.

[53] E. Ribeiro, G. Plantard, J.F. Cornet, F. Gros, C. Caliot, V. Goetz, Experimental and theoretical coupled approaches for the analysis of radiative transfer in photoreactors containing particulate media : case study of TiO2 powders for photocatalytic reactions, Chem. Eng. Sci. 243 (2021) 116733.

[54] W. Oliver, G. Pharr, An improved technique for determining hardness and elastic modulus using load and displacement sensing indentation experiments, J. Mater. Res. 76 (1992) 1564–1583, https://doi.org/10.1557/JMR.1992.1564.

[55] S. Grillo, S. Glénat, T. Tite, O. Pages, O. Maksimov, P. Tamargo, Investigation of the nanomechanical properties in relation to the microstructure of Zn1-xBexTe alloysAppl, Phys. Lett. 93 (2008) 081901, https://doi.org/10.1063/1.2970989.

[56] R. Dimitrijevic, V. Dondur, P. Vulic, S. Markovic, S. Macura, Structural characterization of pure Na-nephelines synthesized by zeolite conversion route, J. Phys. Chem. Solids 65 (10) (2004) 1623–1633.

[57] R. Zhang, S. Xu, D. Raja, N. Khusni, J. Liu, J. Zhang, S. Addulridha, H. Xiang, S. Jiang, Y. Guan, Y. Jiao, X. Fan, On the effect of mesoporosity of FAU zeolites in the liquid phase catalysis, Microporous Mesoporous Mater. 278 (2019) 297.

[58] E. Perez-Botella, S. Valencia, F. Rey, Zeolites in adsorption processes; state of the art and future prospects, Chemical reviews 122 (2022) 17647.

[59] X. Zhang, X. Zhang, X. Li, D. Tian, M. Ma, M. Wang, Optimized pore structure and high permeability of metakaolin/fly-ash-based geopolymer foams from Al– and H2O2–sodium oleate foaming systems, Ceram. Int. 48 (2022) 18348–18360.

[60] X. Deng, J. Wang, S. Du, F. Li, J. Lu, H. Zhang, Fabrication of Porous Ceramics by Direct Foaming, 2014 refractories.

[61] V. Kocí, R. Cerný, Directly foamed geopolymers: a review of recent studies, Cement Concr. Compos. 130 (2022) 104530.

[62] V. Goetz, C. Dezani, E. Ribeiro, C. Caillot, G. Plantard, Continuous flow photocatalytic reactor using TiO2-coated foams, modelling and experimental operating mode, AIChE J. 69 (2023) 17972, https://doi.org/10.1002/aic.17972.

[63] K. Schelm, T. Fey, K. Dammler, U. Betke, M. Scheffler, Hierarchical-porous ceramic foams by a combination of replica and freeze technique, Adv. Eng. Mater. 10 (2019) 155.

[64] A.-C. Derrien, Synthèse et caractérisation physico-chimique de géopolymères et du biomatériau $CaCO_3$ synthétique, Université de Rennes 1, 2004. Thèse de doctorat.

[65] N. Saidi, B. Samet, S. Baklouti, Effect of composition on structure and mechanical properties of metakaolin based PSS-Geopolymer, IJMSCI 3 (4) (2013), https://doi.org/10.14355/ijmsci.2013.0304.03.

[66] T. Luukkonen, M. Sarkkinen, K. Kemppainen, J. Rämö, U. Lassi, Metakaolin geopolymer characterization and application for ammonium removal from model solutions and landfill leachate (2016).

[67] L. Gao, Y. Zheng, Y. Tang, J. Yu, X. Yu, B. Liu, Effect of phosphoric acid content on the microstructure and compressive strength of phosphoric acid-based metakaolin geopolymers, Heliyon 6 (4) (2020) e03853, https://doi.org/10.1016/j.heliyon.2020.e03853.

[68] E. Tkalcec, S. Kurajica, H. Ivankovic, Diphasic aluminosilicate gels with two stage mullitization in temperature range of 1200–1300°C, J. Eur. Ceram. Soc. 25 (5) (2005) 613–626.

[69] A. Autef, E. Joussein, G. Gasgnier, S. Pronier, I. Sobrados, J. Sanz, S. Rossignol, Role of metakaolin dihydroxylation in geopolymer synthesis, Powder Technol. 250 (2013) 33–39.

[70] A. Kaddami, Élaboration et étude des propriétés fonctionnelles de géopolymères moussés, Thèse de Université Paris Est, 2019.

[71] C. Pierlot, H. Hua, C. Reeb, J. Bassetti, M. Bertin, D. Lambertin, C. Davy, Nardello-Rataj, Selection of suitable surfactants for the incorporation of organic liquids, into fresh geopolymer pastes, Chem. Eng. Sci. 255 (2022) 117635.

[72] K. Klima, C.H. Koh, H. Brouwers, Q. Yu, Synergistic effect of surfactants in porous geopolymer: tailoring pore size and pore connectivity, Cement Concr. Compos. 134 (2022) 104774.

[73] A. Gadkar, K. Subramaniam, Porosity and pore structure control in cellular geopolymer using rheology and surface tension modifiers, Construct. Build. Mater. 323 (2022) 126600.

[74] S. Bernal, R. De Gutierrez, S. Delvasto, E. Rodriguez, Performance of an alkali-activated slag concrete reinforced with steel fibers, Constr. Build. Mater. 24 (2010) 208–214, https://doi.org/10.1016/j.conbuildmat.2007.10.027.

[75] D. Dutta, S. Thokchom, P. Ghosh, S. Ghosh, Effect of silica fume additions on porosity of fly ash geopolymers, J. Eng. Appl. Sci. 5 (2010) 74–79.

[76] T.T. Nguyen, H. Bui, T. Ngo, G. Nguyen, Experimental and numerical investigation of influence of air-voids on the compressive behaviour of foamed concrete, Mater. Des. 130 (2017) 103–119, https://doi.org/10.1016/j.matdes.2017.05.054.

[77] G. Ascenscao, M. Seabra, J. Aguiar, J. Labrincha, Red mud-based geopolymers with tailored alkali diffusion properties and pH buffering ability, J. Clean. Prod. 148 (2017) 23e30.

[78] J. Fiset, M. Cellier, P. Vuillaume, Macroporous geopolymers designed for facile polymers post-infusion, Cement Concr. Compos. 110 (2020) 103591.

[79] C. Reeb, C. Pierlot, C. Davy, D. Lambertin, Incorporation of organic liquids into geopolymer materials - a review of processing, properties and applications, Ceram. Int. 47 (2021) 7369–7385.

[80] Rui M. Novais*, RobertC. Pullar, Joao A. Labrincha, Geopolymer foams: an overview of recent advancements, Prog. Mater. Sci. 109 (2020) 100621.

[81] C. Voigt, C. Aneziris, C. alkova, Rheological characterization of slurries for the preparation of alumina foams via replica technique, J. Am. Ceram. Soc. (2015) 1–4, https://doi.org/10.1111/jace.13522.

[82] K. Schelm, E. Abreu Morales, M. Scheffler, Mechanical and surface-chemical properties of polymer derived ceramic replica foams, Materials 12 (2019) 2019, https://doi.org/10.3390/ma12111870.

[83] E. Landi, V. Medri, E. Papa, J. Dedecek, P. Klein, C. Benito, A. Vaccari, Alkali-bonded ceramics with hierarchical tailored porosity, Appl. Clay Sci. 73 (2013) 56–64.

[84] S. Cilla, P. Colombo, M. Morellia, Geopolymer foams by gelcasting, Ceramics International40 (2014) 5723–5730.

[85] T. Janin, V. Goetz, S. Brosillon, G. Plantard, Solar photocatalytic mineralization of 2,4-dichlorophenol and mixtures of pesticides: kinetic model of mineralization, Sol. Energy 87 (2013) 127–135.

[86] G. Plantard, F. Correia, V. Goetz, Kinetic and efficiency of TiO_2-coated on foam or tissue and TiO2-suspension in a photocatalytic reactor applied to the degradation of the 2,4 Diclorophenol, J. Photochem. Photobiol., A 222 (2011) 111–116.

[87] F. Correia, V. Goetz, G. Plantard, S. Sacco, A model for solar photocatalytic mineralization, J. Sol. Energy Eng. 133 (3) (2011) 1–6.

[88] S. Petlitckaia, A. Poulesquen, Design of lightweight metakaolin based geopolymer foamed with hydrogen peroxide, Ceram. Int. (January 2019).